JOURNAL OF MATERIALS SCIENCE 19 (1984) 2064–2072

# Rubber toughening of plastics

## Part 7 *Kinetics and mechanisms of deformation in rubber-toughened PMMA*

CLIVE B. BUCKNALL, IVANA K. PARTRIDGE, MARY V. WARD*
*School of Industrial Science, Cranfield Institute of Technology, Cranfield, Bedford, UK*

Mechanisms of deformation in a series of transparent RTPMMA (rubber-toughened poly(methyl methacrylate)) polymers have been studied by measuring volume changes during creep in tension at 20° C. Volume strains remained small throughout each test, even at total extensions greater than 6%, although the material became heavily stress whitened at strains above about 3%. It was concluded that the dominant mechanism of creep is shear yielding. Rate coefficients, defined by fitting the creep data to the Andrade equation, increase exponentially with applied stress, in accordance with the Eyring equation. Apparent activation volumes increase with rubber content, from 1.55 $nm^3$ for PMMA itself, to 2.89 $nm^3$ for RTPMMA containing 36 vol % of rubber particles. These observations provide an explanation of the toughness and ductility of RTPMMA.

### 1. Introduction

Transparency can be achieved in rubber-toughened glassy polymers, either by matching the refractive index of the rubber with that of the matrix, or by reducing the rubber particle diameter below the wavelength of light [1, 2]. A combination of the two techniques is used commercially to make rubber-toughened poly(methyl methacrylate). The rubber particles are made in emulsion in two or more stages [3]. In a typical two-stage polymer, the rubbery core of the particle consists of a cross-linked copolymer of butyl acrylate, with a minor proportion of styrene; the grafted shell is predominantly PMMA, but may also contain a small amount of a comonomer [4]. Typical particle diameters are about 0.3 $\mu$m. In a three-stage polymer, a rigid core is surrounded by two concentric shells, a rubbery inner shell, and a rigid outer shell consisting essentially of PMMA. The principle can be extended to four or more stages. The core is usually cross-linked to prevent breakdown of the particles during processing. Finally, RTPMMA is made by melt blending composite rubber particles with PMMA.

The toughness of these rubber-modified PMMA materials is in marked contrast to the properties of rubber-modified polystyrene containing particles of the same diameter. The fracture resistance of high-impact polystyrene (HIPS) begins to decrease once the particle size falls below about 1 $\mu$m, an observation that has been attributed to the relative ineffectiveness of small particles in generating crazes [5]. Either the critical particle size for multiple crazing is smaller in RTPMMA than in HIPS, or there is a different mechanism of toughening in RTPMMA that does not operate successfully in HIPS.

The aim of the present programme was to identify the mechanisms of toughening in transparent RTPMMA, and to study the kinetics of the deformation processes, using methods previously applied to other rubber-toughened thermoplastics [6–10]. The basic principle is that crazing and other void-forming processes produce an increase in volume, which enables their contribution to deformation to be distinguished from that of shear yielding, which occurs at approximately constant volume.

*Present address: ICI Petrochemicals and Plastics Division, Wilton, Middlesborough, Cleveland TS6 8JE, UK.


0022–2461/84 $03.00 + .12 

## 2. Experimental procedure

### 2.1. Materials

The transparent RTPMMA materials studied were Oroglas DR100, supplied by Rohm and Haas, and a series of Toughened Diakon polymers, containing various concentrations of rubber particles, supplied by ICI. In each of these materials, the particles appear to have a multi-stage structure, with a hard spherical core surrounded by a rubbery inner shell of cross-linked poly(butyl acrylate-co-styrene) and an outer shell of PMMA. In discussing optical and mechanical properties, the outer shell can be treated as part of the rigid matrix; the toughening particle is effectively the rubbery inner shell and its rigid core, and the values given below for the diameters and volume fractions of rubber particles therefore refer to the effective particle, excluding the outer shell of PMMA. Particle diameters defined in this way were estimated from transmission electron microscopy of thin sections to be approximately 0.3 $\mu$m.

An untoughened injection-moulding grade of PMMA, ICI Diakon MG102, was also included in the programme.

Granules were dried in an oven at 90° C for 5 h, before compression moulding at 190 to 200° C, with 15 min preheating in the mould. Full pressure was applied for about 10 min, and the mould was then water-cooled. Specimens for creep and tensile testing were milled from the resulting 3 mm sheet.

### 2.2. Mechanical tests

Measurements of tensile yield stress were made at $21 \pm 1$° C using a Nene B50 tensometer, over a range of strain rates.

Dumb-bell specimens with a parallel gauge portion 40 mm long and 5 mm wide were conditioned for 3 months at 20° C, before being subjected to creep tests at $20 \pm 0.5$° C, using high-accuracy lever loading rigs. The stresses quoted below are nominal stresses, based on the original cross-sectional area of the specimen. Volume strain $\Delta V$ was calculated from longitudinal strain $\epsilon_3$ and lateral strain $\epsilon_1$, using the equation:

$$\Delta V = (1 + \epsilon_3)(1 + \epsilon_1)^2 - 1 \qquad (1)$$

Each long-term creep test was preceded by a loading–unloading programme at low stresses to determine 100 sec isochronous modulus.

Charpy impact measurements were made over a range of temperatures, on rectangular bars measuring 10 mm x 60 mm, cut from 6.4 mm compression-moulded sheet. A sharp notch 1 mm deep was machined across the narrower face of the bars, which were cooled with the aid of liquid nitrogen, or heated in an air oven, before being removed from this environment and tested in the open laboratory within a few seconds, using a span of 50 mm.

## 3. Results

Results of tensile tests at fixed crosshead speed are presented in Fig. 1. As expected, the unmodified PMMA is relatively brittle; individual crazes are formed on planes perpendicular to the tensile axis as the stress approaches 40 MPa, and the material then fractures at a strain of about 3%. By contrast, the RTPMMA materials begin to show a hazy whitening at strains of about 3%, which intensifies as stress and strain increase up to the yield point, and continues beyond yield, tending to become concentrated into broad bands lying at 45° to the tensile axis, until most of the parallel gauge portion is densely whitened. Specimens reach strains of up to 30% without necking. Both the yield stress $\sigma_y$ and the magnitude of the yield drop, increase with increasing strain rate $\dot{\epsilon}$. As illustrated in Fig. 2, the strain rate dependence of yield stress can be represented by the Eyring equation:

$$\sigma_y = \frac{kT}{\gamma V} \log_e \frac{\dot{\epsilon}}{A} \qquad (2)$$

where $k$ is Boltzmann's constant, $T$ temperature, $\gamma$ a stress concentration factor, $V$ activation volume and $A$ a constant.

Modulus data obtained from 100 sec creep tests are presented in Fig. 3. Non-linear viscoelastic behaviour is observed in all of the materials tested, the decrease in modulus with strain being especially marked at strains above about 1%. The relationship between modulus and effective volume fraction of rubber particles is shown in Fig. 4.

Typical creep and recovery curves for PMMA and RTPMMA are shown in Fig. 5. In both materials there is a rapid response on applying the load, followed by time-dependent extension at a decreasing rate. Neither material shows any significant increase in volume with time, and it is clear that the principal mechanism of creep is shear deformation. Small errors in lateral and longitudinal strains $\epsilon_1$ and $\epsilon_3$ can have a disproportionately

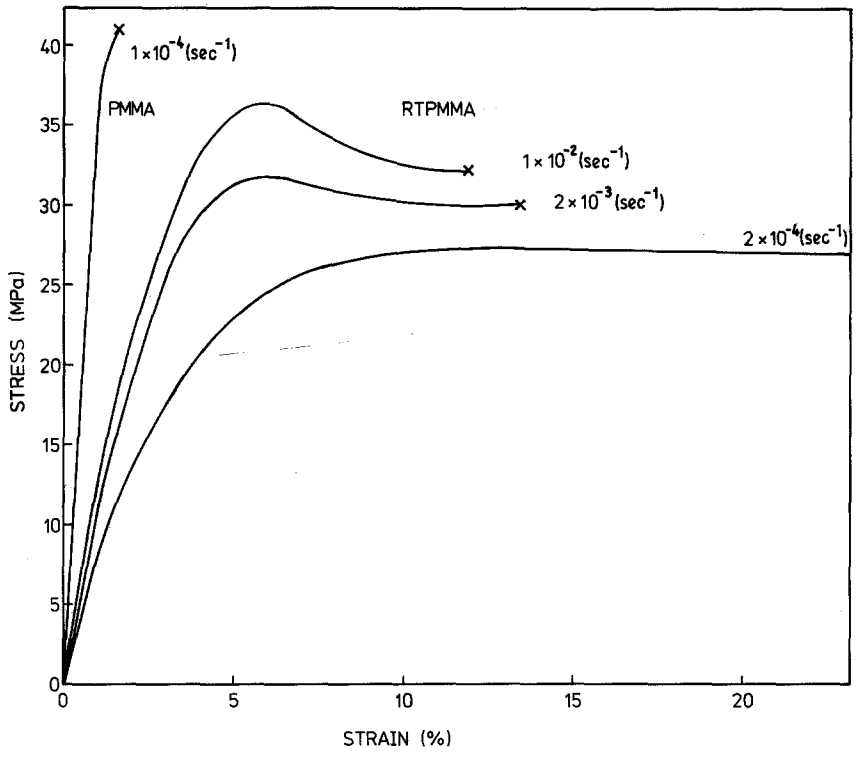


*Figure 1* Effect of strain rate on yield behaviour of RTPMMA containing 36 vol % of rubber particles.

large effect upon the calculated value of volume strain $\Delta V$, especially when $\epsilon_1$ and $\epsilon_3$ are both large, so that the slight upward trend in $\Delta V$ in Fig. 5b does not provide conclusive proof of dilatation in the RTPMMA. The difference in mechanism between RTPMMA and the styrene-based polymers HIPS and ABS is emphasized in Fig. 6: a slope of 1.0 in the graph of volume strain against elongation is characteristic of a material in which crazing is the dominant mechanism of creep, whereas a slope of zero indicates that there is little or no crazing or void formation. In all tests carried out on PMMA and RTPMMA, the slope was close to zero, clearly showing that shear processes are predominant in the time-dependent creep response of these materials over the range of strains and strain rates studied in this programme. Optical, scanning electron and transmission electron microscopy showed no evidence of crazing, even in the most densely whitened zones.

The relationship between extension $\epsilon(t)$ and time $t$ can be expressed to a good approximation by the Andrade equation:

$$\epsilon = \epsilon(t) - \epsilon(0) = (Bt)^{1/3} \qquad (3)$$

where $\epsilon(0)$ is the strain at time zero, immediately after loading, and $B$ is a rate coefficient, having the dimensions of reciprocal time. Andrade plots for PMMA and one of the RTPMMA materials are presented in Fig. 7.

It can be seen that the strain is linear with the cube root of time, up to a strain of 5%, beyond which there are indications of more rapid creep. A possible reason for this change in the kinetics is the small increase in true stress resulting from the decreasing cross-sectional area of the specimen.

The increase in the rate coefficient $B$ with applied stress is shown in Fig. 8 in the form of an Eyring plot, using a rearranged form of Equation 2:

$$B = A \exp\left(\frac{\gamma V \sigma}{kT}\right) \qquad (4)$$

$$\log_e \frac{B}{A} = \frac{\gamma V \sigma}{kT} \qquad (5)$$

The results show that $\gamma V$ increases with increasing rubber content. On the assumption that the activation volume $V$ is a characteristic of the shear yielding process in PMMA, and has the same value in all three materials, it follows that the increasing slope is a measure of the effective stress concentration factor $\gamma$ in the region undergoing shear deformation, which must obviously increase with rubber content.

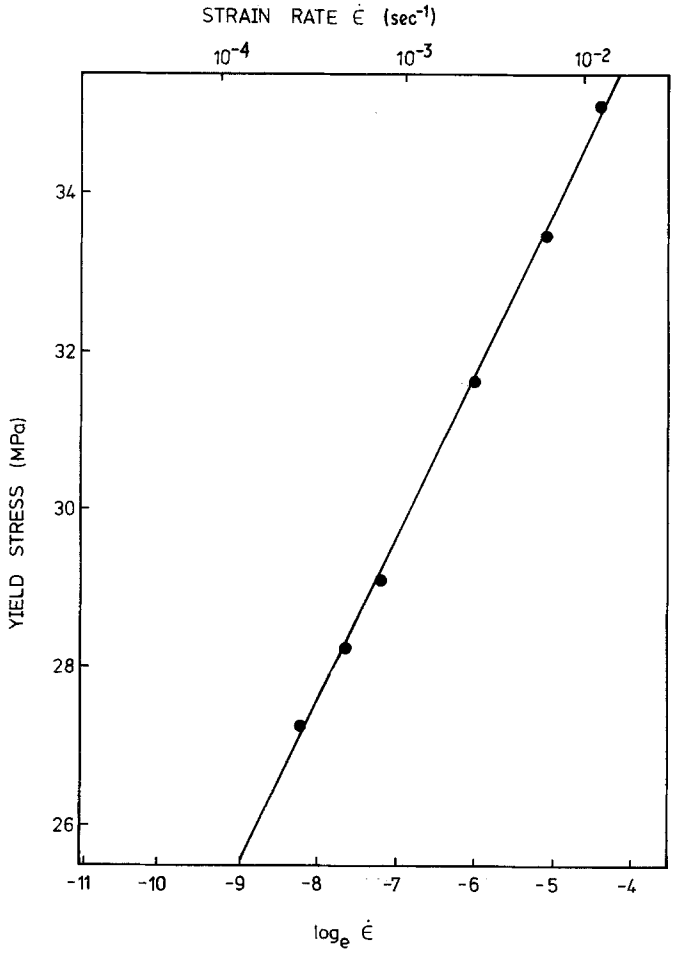


*Figure 2* Eyring plot of yield stress against log strain rate for RTPMMA containing 36 vol% rubber particles.

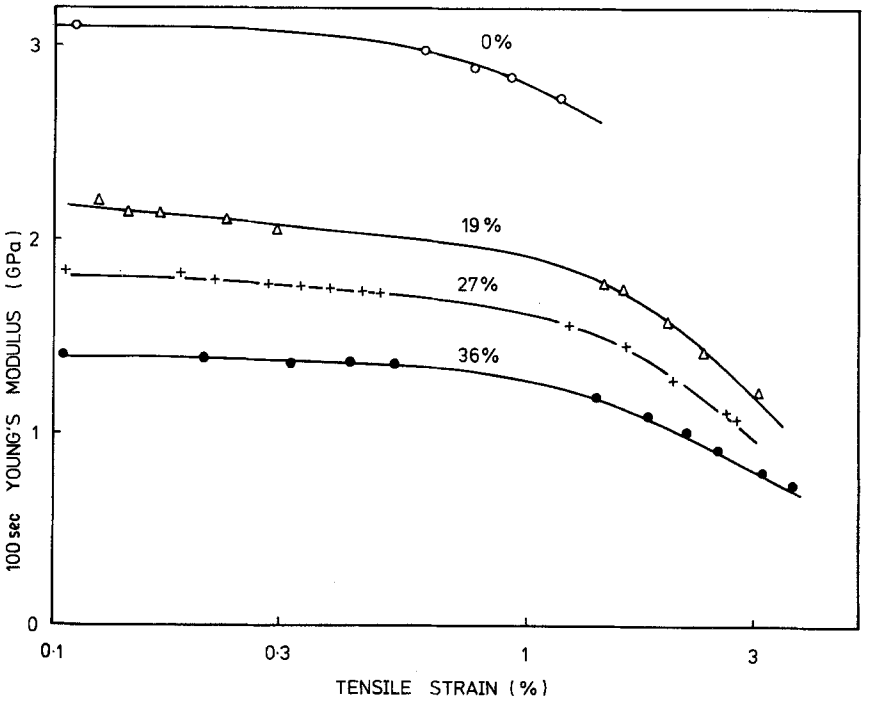


*Figure 3* Modulus data for PMMA and RTPMMA.

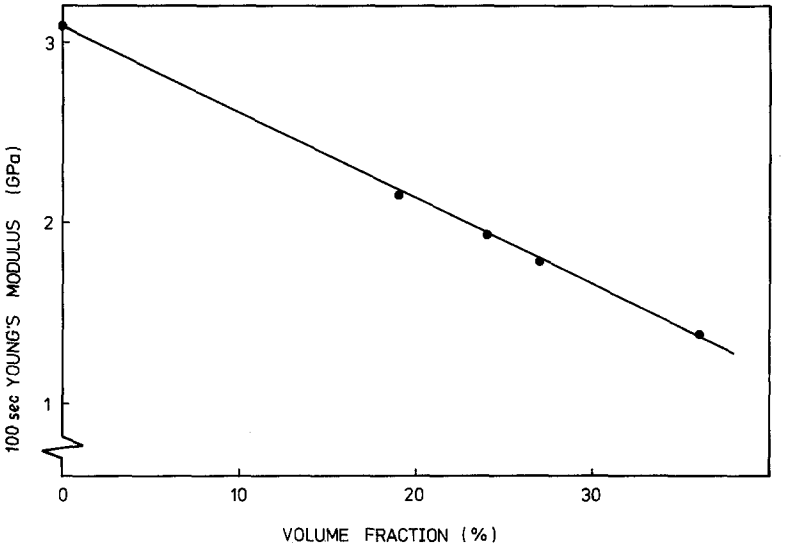


*Figure 4* Relationship between 100 sec modulus at 0.1% strain and effective volume fraction of rubber.

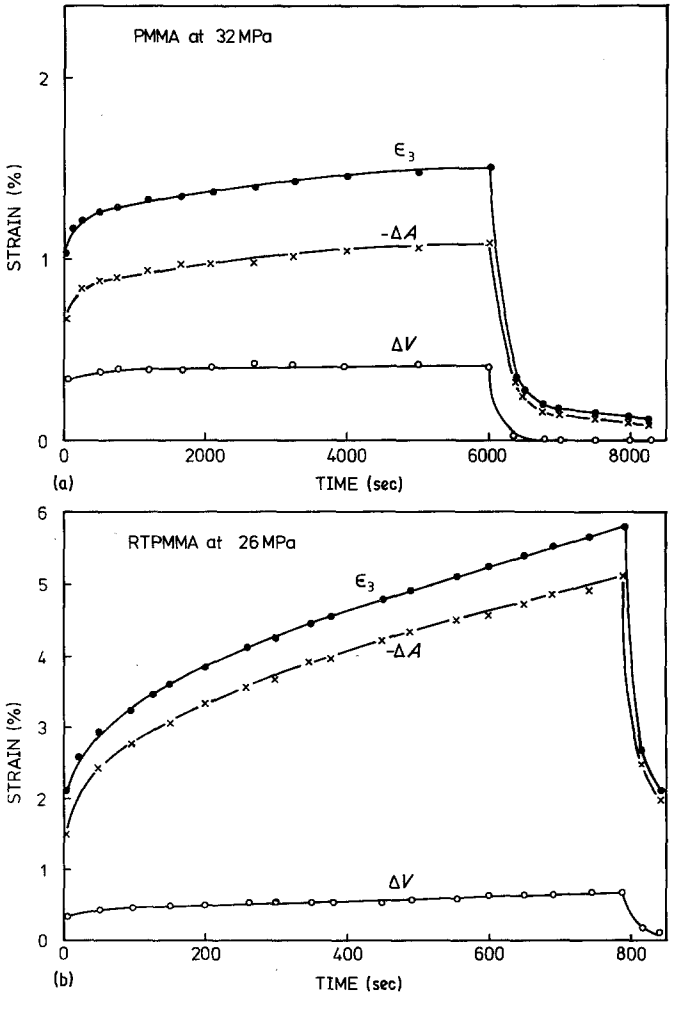


*Figure 5* Creep and recovery curves showing extension $\epsilon_3$, area strain $\Delta A$ and volume strain $\Delta V$ for (a) PMMA; and (b) RTPMMA containing 36 vol% rubber particles.

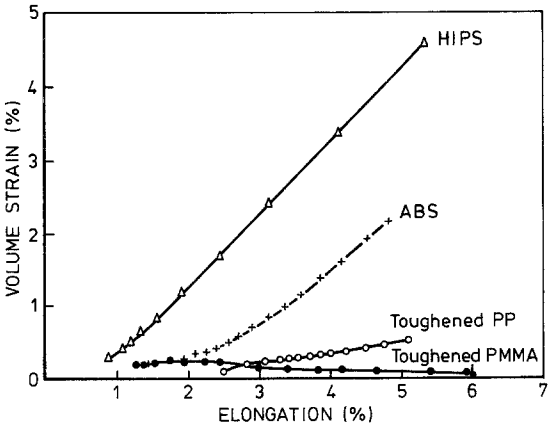


*Figure 6* Relationship between volume and axial strain in creep, showing differences in mechanisms of deformation between different rubber-toughened polymers.

Charpy impact results for sharply-notched specimens are shown in Fig. 9. Rubber modification has little effect on fracture resistance below $-10^\circ$ C, but there is a marked rise in impact between $-5$ and $+23^\circ$ C, and a further sharp rise above $23^\circ$ C. Corresponding changes can be seen on the fracture surfaces of RTPMMA specimens. Below $-5^\circ$ C, the surfaces are rough and broken, like those of PMMA itself. Between $-5$ and $23^\circ$ C, a relatively flat area, showing a faint bluish tinge, forms next to the notch, whilst the remainder of the surface is again rough and broken. The size of this flat area increases with temperature, until at $30^\circ$ C and above it occupies the entire fracture surface. A similar pattern of behaviour has been observed previously in other rubber-modified plastics, notably HIPS and ABS (acrylonitrile–butadiene–styrene) [12, 13]. The first transition in properties, at about $-10^\circ$ C, is clearly associated with the glass transition in the elastomeric region of the composite rubber particles; the second transition can also be regarded as associated with the $T_g$ of the rubber particles, but now shifted to about $25^\circ$ C in accordance with the time–temperature superposition principle, as the crack gathers speed and the time scale of the required response is reduced [12]. The faint blue tinge mentioned earlier indicated that the depth below the fracture surface of the visible yield zone is smaller in RTPMMA than in many other rubber-modified polymers tested under similar conditions; a dense whitening is usually seen in ABS, for example.

## 4. Discussion

These experiments clearly show that shear yielding is the dominant mechanism of deformation in the

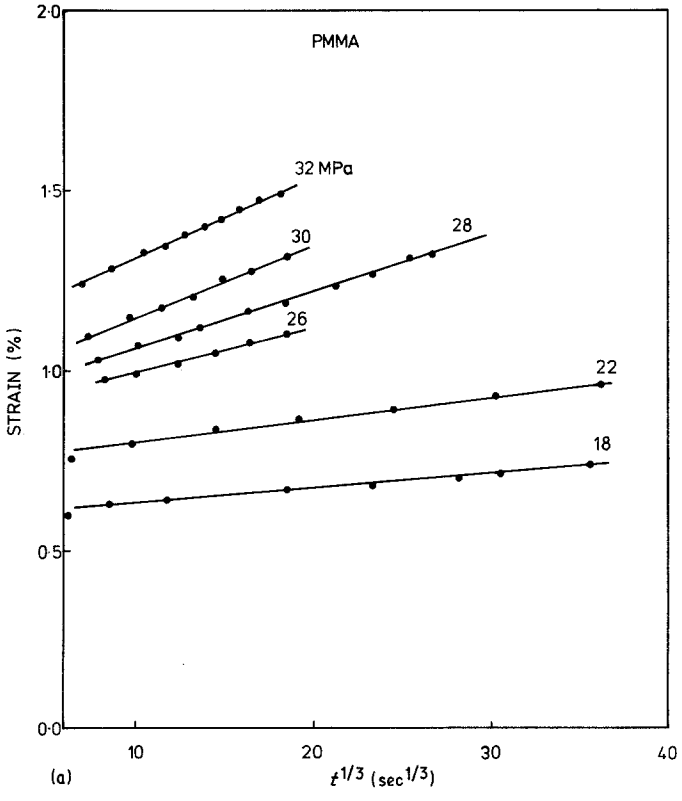


*Figure 7* Andrade plots for (a) PMMA and (b) RTPMMA containing 27 vol% of rubber particles.

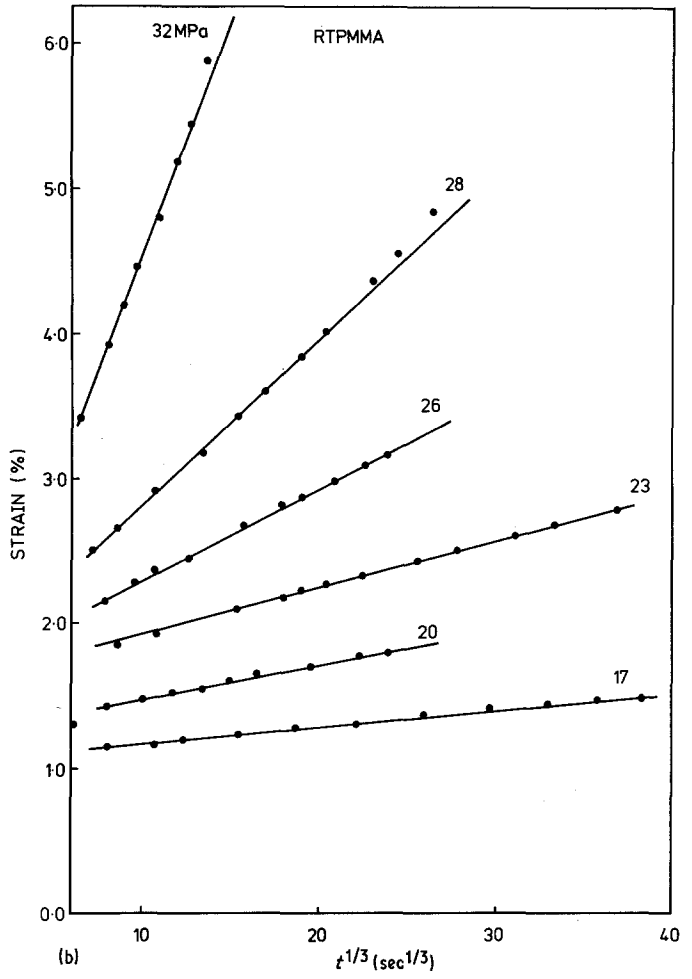


*Figure 7* Continued.

rubber-toughened PMMA materials studied in this programme. This conclusion is based on the evidence of creep experiments, in which it is observed that the material deforms from an initial tensile strain of about 1% to at least 6%, without significantly increasing in volume. Hooley and co-workers reached a similar conclusion on the basis of a more limited study of volume changes in RTPMMA during deformation at constant strain rate [3]. Additional evidence has been obtained by Bucknall and Marchetti, who showed that RTPMMA developed an expanded elliptical

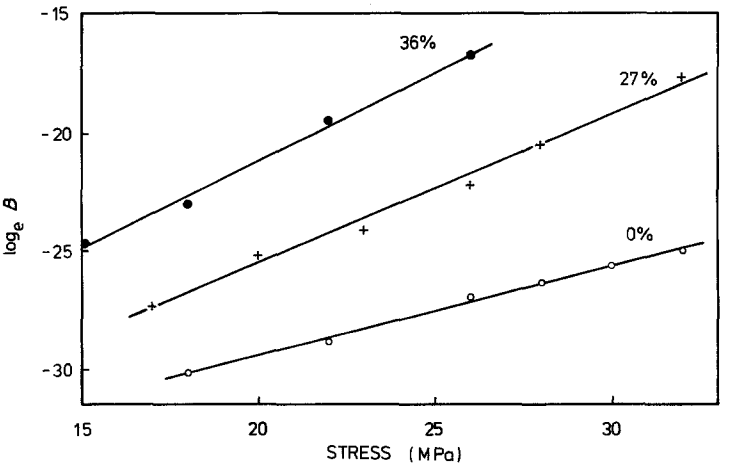


*Figure 8* Eyring plots of Andrade rate parameter $B$ against stress for PMMA containing various concentrations of rubber particles.

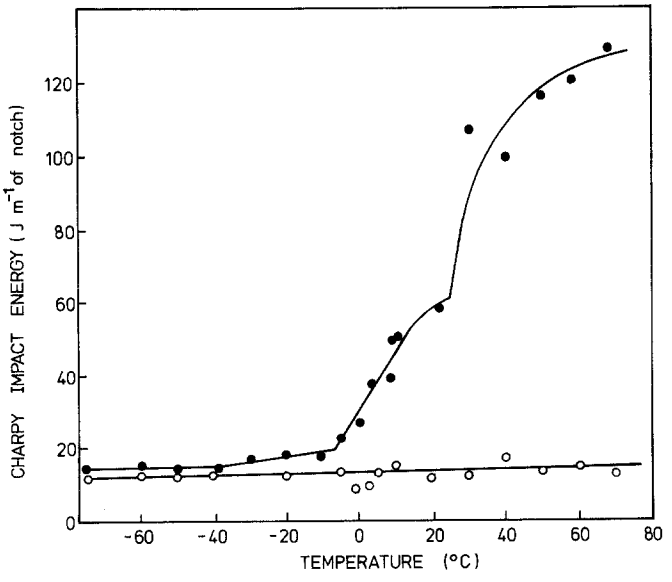


*Figure 9* Relationship between razor-notched Charpy impact energy and temperature for PMMA and RTPMMA containing 36 vol% of rubber particles.

hysteresis loop during sinusoidal tension–compression cycling [14], and that a similarly-shaped expanded loop was observed on load-cycling a specimen, prestrained in tension almost to the point of fracture [15]. Symmetrical hysteresis loops of this type are characteristic of shear yielding: the loops formed in strained HIPS, which deforms by multiple crazing, are highly assymmetrical and distinctive in shape [16]. The evidence that shear yielding is the principal mechanism of energy absorption in the Charpy impact specimens is less conclusive, but it should be noted that the fracture surfaces do not show the dense whitening usually seen in materials that deform by multiple crazing, and that any whitening would be much easier to observe in transparent RTPMMA than in a typical HIPS.

The PMMA materials are similar to polypropylenes, which also shear yield, in following Andrade kinetics to a sufficiently good approximation, to enable a rate coefficient to be defined at each stress level [10]. Differentiation of Equation 3 gives:

$$\frac{d\epsilon}{dt} = \frac{B}{3\epsilon^2} \tag{6}$$

which defines $B$ as the rate coefficient for the process. Apparent activation volumes, $\gamma V$, determined from the data given in Fig. 8, are 1.55 nm$^3$ for PMMA containing no rubber, 2.53 nm$^3$ for RTPMMA containing 27 vol% of composite rubber particles, 2.89 nm$^3$ for the material containing 36 vol% of rubber particles, and 2.28 nm$^3$ for Oroglas DR100, which contains a different PMMA matrix polymer from the other materials. On the assumption that the activation volume $V$ for shear yielding in PMMA is the same in each of the first three materials, these figures mean that the stress concentration factor $\gamma$ in RTPMMA is 1.63 at a rubber particle loading of 27 vol% and 1.86 at a loading of 36 vol%.

These values for $\gamma$ are lower than might have been expected, especially in view of the high volume fractions of rubber particles. Nevertheless, they reflect a substantial increase in creep rate at a given stress, or, conversely, a decrease in yield stress at a given strain rate. This ability of the rubber particle to reduce yield stress is an important part of their function in increasing fracture resistance. Equally important is their capacity to deform with the surrounding matrix after it has yielded, so that the stress is redistributed; in this respect, rubber particles appear to be unique. Both functions are lost when the rubber is below its glass transition, and the RTPMMA is therefore brittle at low temperatures.

In view of the observation that volume changes are minimal during creep of RTPMMA, the dense stress whitening requires an explanation. One possibility is that volumetric strains developed in the rubber phase as a result of shear yielding in the matrix are sufficient to cause a drop in the refractive index of the rubber particles, so that it no longer matches that of the matrix. Another possibility is that voids form at some suitable nucleus, which might be within the rubber phase,

or at the particle–matrix interface, or at the intersection of two shear bands in the matrix. Attempts to resolve this point using electron microscopy have so far proved unsuccessful. Light scattering techniques might be more informative in this case.

The difference in mechanisms of deformation between these transparent RTPMMA polymers and a typical HIPS is striking, especially as both matrix polymers are brittle, glassy materials having $T_g$s at about 100° C. It is clearly a question of balance, since both polystyrene and poly(methyl methacrylate) will craze and shear yield under appropriate conditions. The extent to which this balance is affected by (a) the size and internal structure of the rubber particles and (b) the chemical constitution, molecular weight distribution, and thermal history of the matrix, remains to be determined. The available evidence suggests that each of these factors is important in its own way.

## Acknowledgements

The authors would like to express their thanks to the Science and Engineering Research Council for a grant in support of this work, to ICI for a studentship awarded to MVW, and to ICI and Rohm and Haas for the gift of materials.

## References

1. B. F. CONAGHAN and S. L. ROSEN, *Polym. Eng. Sci.* **12** (1972) 134.
2. C. B. BUCKNALL, "Toughened Plastics" (Applied Science, London, 1977) p. 50.
3. C. J. HOOLEY, D. R. MOORE, M. WHALE and M. J. WILLIAMS, *Plast. Rubber Process. Appl.* **1** (1981) 345.
4. BP **1**, 340, 025.
5. G. MICHLER, *Plast. Kaut.* **26** (1979) 497, 680.
6. C. B. BUCKNALL and D. CLAYTON, *J. Mater. Sci.* 7 (1972) 202.
7. C. B. BUCKNALL, D. CLAYTON and W. E. KEAST, *ibid.* 7 (1972) 1443.
8. *Idem, ibid.* 8 (1973) 514.
9. C. B. BUCKNALL and I. C. DRINKWATER, *ibid.* 8 (1973) 1800.
10. C. B. BUCKNALL and C. J. PAGE, *ibid.* **17** (1982) 808.
11. A. S. KRAUSZ and H. EYRING, "Deformation Kinetics" (Wiley, New York, 1975).
12. C. B. BUCKNALL, "Toughened Plastics" (Applied Science, London, 1977) p. 290.
13. L. V. NEWMANN and J. G. WILLIAMS, *Polym. Eng. Sci.* **18** (1978) 893.
14. C. B. BUCKNALL and A. MARCHETTI, *J. Appl. Polym. Sci.* **28** (1983) 2689.
15. *Idem, Polym. Eng. Sci.* in press.
16. C. B. BUCKNALL and W. W. STEVENS, *J. Mater. Sci.* **15** (1980) 2950.

*Received 6 September*
*and accepted 22 September 1983*